LETTER

doi:10.1038/nature20145

Neuromodulators signal through astrocytes to alter neural circuit activity and behaviour

Zhiguo Ma[1], Tobias Stork[1], Dwight E. Bergles[2] & Marc R. Freeman[1]†

Astrocytes associate with synapses throughout the brain and express receptors for neurotransmitters that can increase intracellular calcium (Ca^{2+})[1–3]. Astrocytic Ca^{2+} signalling has been proposed to modulate neural circuit activity[4], but the pathways that regulate these events are poorly defined and *in vivo* evidence linking changes in astrocyte Ca^{2+} levels to alterations in neurotransmission or behaviour is limited. Here we show that *Drosophila* astrocytes exhibit activity-regulated Ca^{2+} signalling *in vivo*. Tyramine and octopamine released from neurons expressing tyrosine decarboxylase 2 (Tdc2) signal directly to astrocytes to stimulate Ca^{2+} increases through the octopamine/tyramine receptor (Oct-TyrR) and the transient receptor potential (TRP) channel Water witch (Wtrw), and astrocytes in turn modulate downstream dopaminergic neurons. Application of tyramine or octopamine to live preparations silenced dopaminergic neurons and this inhibition required astrocytic Oct-TyrR and Wtrw. Increasing astrocyte Ca^{2+} signalling was sufficient to silence dopaminergic neuron activity, which was mediated by astrocyte endocytic function and adenosine receptors. Selective disruption of Oct-TyrR or Wtrw expression in astrocytes blocked astrocytic Ca^{2+} signalling and profoundly altered olfactory-driven chemotaxis and touch-induced startle responses. Our work identifies Oct-TyrR and Wtrw as key components of the astrocytic Ca^{2+} signalling machinery, provides direct evidence that octopamine- and tyramine-based neuromodulation can be mediated by astrocytes, and demonstrates that astrocytes are essential for multiple sensory-driven behaviours in *Drosophila*.

Astrocytes are intimately associated with brain synapses and positioned to broadly regulate synaptic activity. It has been widely proposed that astrocytes modulate neural circuits and behaviour[5–7], although *in vivo* evidence that astrocytes are directly activated by neurotransmission and signal back to neurons to modulate their output remains elusive. Astrocytes exhibit dynamic fluctuations in intracellular Ca^{2+} *in vitro*[8,9] and *in vivo*[10,11], suggesting that Ca^{2+} signalling might be a useful measure of astrocytic activity. Despite decades of studies on astrocytic Ca^{2+} transients, the signalling pathways that control these transients remain poorly defined, and their *in vivo* relevance remains controversial. If astrocytes actively participate in information processing in circuits, it is imperative that we characterize the mechanisms involved as they would represent a potentially widespread mechanism for controlling brain function.

We performed an RNA interference (RNAi)-based screen in *Drosophila* in which we individually knocked down around 500 Ca^{2+} signalling-related genes selectively in astrocytes using the astrocyte-specific *Gal4* driver line *alrm–Gal4* (ref. 12), and assayed larval olfactory-driven chemotaxis (Extended Data Fig. 1a). We found that astrocyte knockdown of the TRP channel Wtrw[13] led to a significant (~50%; $P < 0.01$) decrease in larval chemotaxis towards iso-amyl acetate (IAA) (Fig. 1a). Similar results were found with a second, non-overlapping RNAi construct (Fig. 1a); the effect of Wtrw knockdown was specific to glia, as shown by insensitivity to blockade of Gal4/UAS in neurons expressing *elav–Gal80* (Extended Data Fig. 1e). Larvae bearing the null allele $wtrw^{ex}$ were equally defective in chemotaxis, but this behaviour was rescued by re-expression of *wtrw* only in astrocytes (Fig. 1a). We also found that blockade of Gal4/UAS-driven $wtrw^{RNAi}$ with *tsh–Gal80* in the ventral nerve cord (VNC) resulted in normal chemotaxis responses (Extended Data Fig. 1d, f), revealing a critical role for VNC astrocytes in this behaviour, although this does not exclude an additional role for brain astrocytes. Chemotaxis defects did not result from simple alterations in motility, as $wtrw^{RNAi}$ larvae exhibited normal locomotion (Extended Data Fig. 1g) and light avoidance responses (Extended Data Fig. 1c, h). We conclude that Wtrw is required in astrocytes for normal larval olfactory-driven behaviour.

Ca^{2+} transients are induced in astrocytes in awake behaving mice during periods of elevated arousal[14–16]. We therefore used a gentle anterior touch assay[17] to investigate the role of astrocyte Ca^{2+} signalling in larval startle-induced behaviours. Crawling larvae touched anteriorly with a hair responded by pausing and continuing forwards (type I response), or by moving backwards and executing an escape response (type II response; Extended Data Fig. 1b). Wild-type larvae and controls without RNA knockdown exhibited roughly equal frequencies of type I and type II responses, but the expression of $wtrw^{RNAi}$ in astrocytes resulted in a marked alteration in behaviour: about 80% of larvae exhibited type I responses. This phenotype was mimicked by $wtrw^{ex}$ mutants (Fig. 1b) and was independent of neuronal Wtrw expression (Extended Data Fig. 1i). These data indicate that astrocyte-expressed Wtrw also modulates startle-induced behavioural changes in *Drosophila* larvae.

To study *in vivo* Ca^{2+} signalling, we developed a semi-dissected preparation to image the larval CNS. We used the fluorescent calcium sensor GCaMP6s to image astrocyte cytosolic Ca^{2+} changes (UAS–GCaMP6s) and mCherry (UAS–mCherry) as a reference for astrocyte position, and imaged dorsal astrocyte cell bodies in the VNC. Astrocyte cell bodies exhibited coordinated, population-wide slow oscillations (termed somatic Ca^{2+} transients; Extended Data Fig. 1j–l and Supplementary Video 1). Somatic Ca^{2+} transients occurred approximately every 2 min and exhibited an average change in $\Delta F/F$ of about 11% (Extended Data Fig. 1m). Notably, blocking neuronal activity with tetrodotoxin (TTX) suppressed transients by approximately 60%, as did application of the broad Ca^{2+} channel blocker lanthanum chloride ($LaCl_3$; Extended Data Fig. 1n). Similar astrocytic Ca^{2+} transients were observed when we imaged intact immobilized larvae (Extended Data Fig. 1o), indicating that our dissected preparation preserves *in vivo* patterns of astrocyte activity.

TRP channels regulate Ca^{2+} levels in astrocytes[18], so we reasoned that Wtrw might drive Ca^{2+} signalling in *Drosophila* astrocytes. Wild-type larvae exhibited 8–9 rhythmic oscillations in somatic Ca^{2+} transients over 15 min. By contrast, astrocyte-specific $wtrw^{RNAi}$ led to a roughly 50% decrease in somatic astrocyte Ca^{2+} transients, which was also observed in the $wtrw^{ex}$ mutant (Fig. 1c). Bath application of

[1]Department of Neurobiology and Howard Hughes Medical Institute, University of Massachusetts Medical School, Worcester, Massachusetts 01605, USA. [2]Solomon H. Snyder Department of Neuroscience, Johns Hopkins University School of Medicine, Baltimore, Maryland 21205, USA. †Present address: Vollum Institute, Oregon Health and Sciences University, Portland, Oregon 97239, USA.

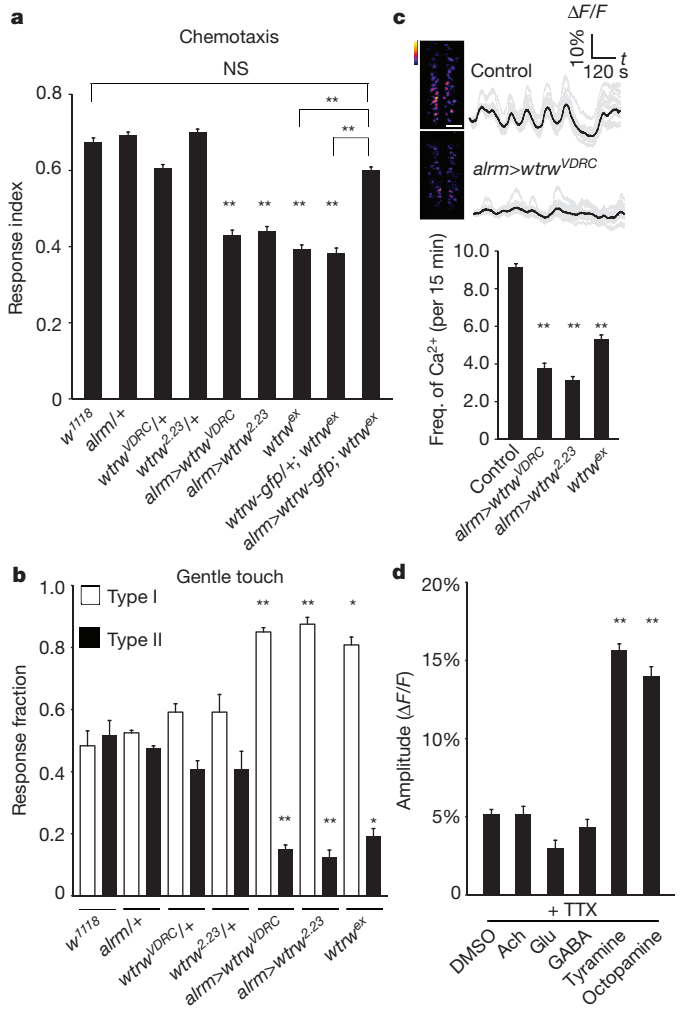

Figure 1 | Larval chemotaxis and startle-induced responses require the astrocyte-expressed TRP channel Wtrw. a, Chemotaxis assay ($n = 12$). **b**, Gentle touch assay ($n = 30$). **c**, Pseudocoloured maximum intensity projections of 15-min movies, averaged traces of 16 individual astrocytes and quantifications of the frequency of somatic Ca^{2+} transients ($n = 10$, 160 cells total). Scale bar, 50 μm. **d**, Responses of astrocytes to neurotransmitters and neuromodulators in the presence of TTX ($n = 6$, 96 cells total). $*P < 0.05$, $**P < 0.01$; NS, not significant; error bars, s.e.m. **a**, Wilcoxon and Mann–Whitney tests followed by Bonferroni-Holm *post hoc* test; **b**–**d**, One-way ANOVA followed by Tukey's *post hoc* test. Ach, acetylcholine; GABA, γ-aminobutyric acid; Glu, glutamate.

acetylcholine, glutamate, or γ-aminobutyric acid in the presence of TTX did not elicit a change in Ca^{2+} levels in astrocytes. By contrast, application of tyramine (Tyr) or octopamine (Oct), the invertebrate analogues of norepinephrine, which has been shown to induce Ca^{2+} transients in mammalian astrocytes[14,15,19,20], potently elevated somatic Ca^{2+} in astrocytes (Fig. 1d), indicating that astrocyte somatic Ca^{2+} signalling is regulated by these neuromodulators.

$Tdc2^+$ neurons are the only known source of Tyr and Oct in the larval VNC[21]. To investigate the relationship of these neurons with astrocytes we expressed the red-shifted Ca^{2+} indicator R-GECO1 in $Tdc2^+$ neurons (using *tdc2-LexA/LexAop-R-GECO1*) and GCaMP6s in astrocytes (using *alrm-Gal4/UAS-GCaMP6s*) and examined *in vivo* activity. We observed a striking positive correlation between $Tdc2^+$ neuron activity and somatic astrocyte Ca^{2+}: when $Tdc2^+$ neurons were active, astrocyte somatic Ca^{2+} levels increased, and when $Tdc2^+$ neurons were silent, astrocyte somatic Ca^{2+} levels decreased (Fig. 2a and Supplementary Video 2). A similar correlation was observed in intact larvae (Extended Data Fig. 1p). Moreover, the amplitude and duration of the increase in somatic astrocyte Ca^{2+} was tightly correlated with Ca^{2+} spikes in $Tdc2^+$ neurons (Fig. 2a). When we chronically silenced $Tdc2^+$ neurons by expressing the K^+ leak channel Kir2.1 (ref. 22), rhythmic oscillations in astrocyte Ca^{2+} were eliminated (Fig. 2b and Extended Data Fig. 2a); in addition, acute optogenetic blockade of $Tdc2^+$ neuron activity using halorhodopsin (*tdc2-Gal4> UAS-NpHR*) led to a decrease in astrocyte somatic Ca^{2+} (Fig. 2c and Extended Data Fig. 2b). Notably, astrocytic Ca^{2+} signalling was also blocked by the α1 adrenergic receptor antagonist terazosin (Fig. 2d and Extended Data Fig. 2c), which inhibits arousal-evoked Ca^{2+} responses in cortical astrocytes in mammals[14,15], further supporting the notion that astrocyte modulation is highly conserved between species. Consistent with astrocyte Ca^{2+} signalling being regulated by Oct and Tyr, somatic astrocyte Ca^{2+} transients were nearly absent (about 80% reduced) in $tdc2^{RO54}$ mutants, which lack both Tyr and Oct, although they persisted in $t\beta h^{nM18}$ mutants, which lack Oct but retain Tyr signalling (Fig. 2e, f). Finally, $Tdc2^+$ neurons were activated when olfactory neurons were optogenetically stimulated in intact larvae (using *or83b-Gal4*), suggesting that sensory cues flow to $Tdc2^+$ neurons, which are upstream of astrocyte Ca^{2+} signalling (Extended Data Fig. 2d).

To determine whether $Tdc2^+$ neurons signal directly to astrocytes we knocked down the two Tyr receptors, TyrR and TyrRII, and Oct-TyrR, a dual specificity receptor that can bind both Oct and Tyr[23,24], in astrocytes and assayed Ca^{2+} signalling. Depletion of TyrR or TyrRII had no effect (data not shown), but depletion of Oct-TyrR strongly suppressed astrocyte somatic Ca^{2+} transients. We observed strong inhibition of astrocyte somatic Ca^{2+} transients in the $Oct\text{-}TyrR^{hono}$ homozygous mutant, and in $Oct\text{-}TyrR^{hono}/+$ heterozygous mutants, which were previously shown to have dominant effects[25] (Fig. 2g). Loss of one copy of *Oct-TyrR* ($Oct\text{-}TyrR^{hono}/+$) also led to defects in chemotaxis behaviour similar to those observed after astrocyte-specific knockdown of *wtrw*; these behavioural changes were enhanced in the $Oct\text{-}TyrR^{hono}$ homozygous mutant, or by astrocyte-specific knockdown of *Oct-TyrR* with two copies of an *Oct-TyrR* RNAi construct. Co-expression of $Oct\text{-}TyrR^{RNAi}$ and $wtrw^{RNAi}$ did not enhance chemotaxis defects, suggesting that Oct-TyrR and Wtrw act in a common genetic pathway (Fig. 2h). Finally, astrocyte-specific depletion of Oct-TyrR led to strong inhibition of type II escape responses in the gentle anterior touch assay (Fig. 2i). We conclude that Wtrw and Oct-TyrR are required in astrocytes to trigger somatic Ca^{2+} transients in response to Oct and Tyr, and astrocytic Wtrw and Oct-TyrR are essential for normal olfactory-driven chemotaxis and startle-induced escape responses.

Astrocytes support neuronal function in many ways and it is plausible that alterations in astrocyte Ca^{2+} signalling might modify upstream $Tdc2^+$ neuron firing to influence behaviour. We therefore measured the frequency and amplitude of firing events in $Tdc2^+$ neurons in $wtrw^{ex}$ null mutants and found no alterations compared to wild-type controls (Extended Data Fig. 2e). That $Tdc2^+$ neurons fire normally in *wtrw* mutants indicates that blocking astrocytic Ca^{2+} signalling does not lead to a global disruption of neuronal activity in the larval CNS.

Biogenic amines often regulate dopaminergic neurons[26]. Triple labelling revealed that astrocytes, $Tdc2^+$ neurons and dopaminergic neurons are in close proximity in the larval CNS (Extended Data Fig. 2f). When we imaged dopaminergic neuron activity (using *th-Gal4/UAS-GCaMP6s*) we found that $wtrw^{ex}$ mutants exhibited a significant increase (about 50–70%; $P < 0.01$ for t1, $P < 0.05$ for t2 and t3) in the frequency of dopaminergic Ca^{2+} transients in multiple segmental clusters of tyrosine hydroxylase $(TH)^+$ cells. A similar phenotype was observed in $Oct\text{-}TyrR^{hono/+}$ mutants (Fig. 3a), although there were no significant changes in the average amplitude of dopaminergic neuron responses (Extended Data Fig. 2g). Thus Wtrw and Oct-TyrR negatively regulate dopaminergic neuron firing. Consistent with this observation, bath application of Oct or Tyr, but not vehicle (DMSO), to the larval CNS suppressed dopaminergic neuron activity within seconds (Fig. 3b). Strikingly, depletion of the Oct-TyrR and Wtrw specifically from astrocytes using RNAi potently suppressed Tyr-induced Ca^{2+}

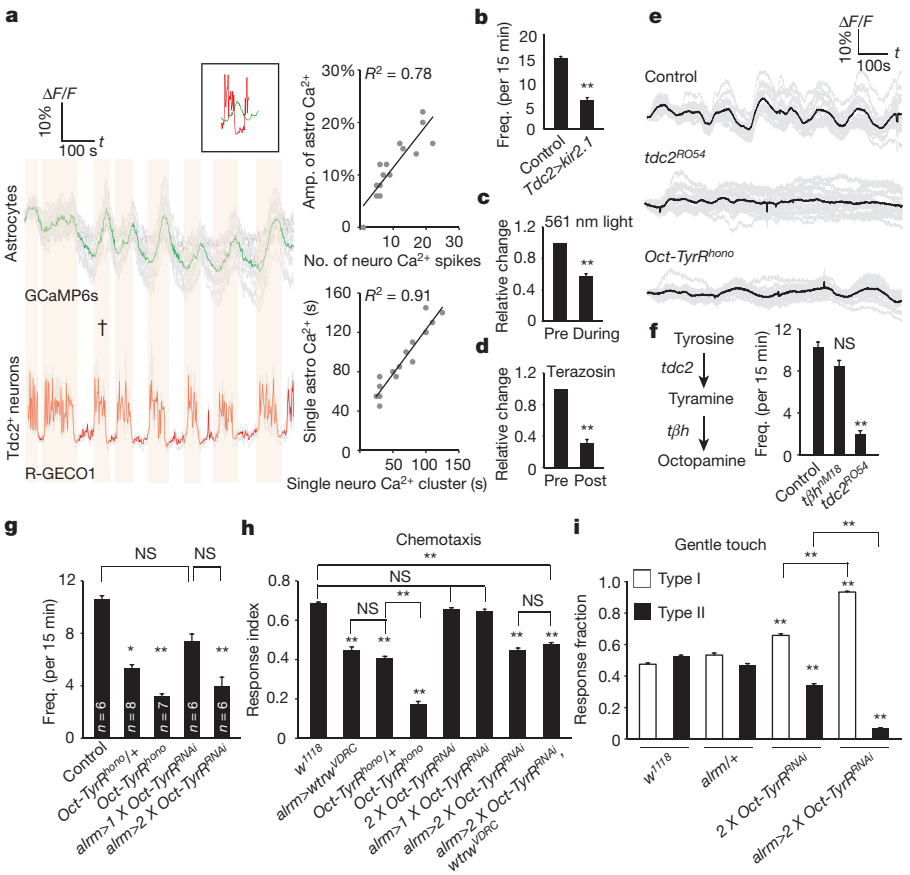

Figure 2 | Tdc2^{+} neurons fire rhythmically to drive astrocyte somatic Ca^{2+} transients through the Oct-TyrR. a, Correlation analyses of neuronal activity and somatic Ca^{2+} transients in astrocytes. Averaged traces of 16 individual astrocytes (GCaMP6s) and 4 pairs of Tdc2^{+} neurites (R-GECO1) from the same sample. Vertical orange bars highlight concomitant activity in astrocytes and neurons (†events shown in inset). Amplitude and duration of individual Ca^{2+} transients in astrocytes correlate highly with activity of Tdc2^{+} neurons. **b**, Frequency of Ca^{2+} transients in astrocytes ($n = 10$, 160 cells total). **c**, **d**, Relative changes in numbers of Ca^{2+} transients after acute blockade of Oct and Tyr signalling by halorhodopsin (**c**) or terazosin (**d**) ($n = 6$, 96 cells total). Black dots denote points at which either 561 nm light or terazosin was administered. **e**, Representative traces of astrocytic Ca^{2+} transients in mutants defective in Oct and Tyr signalling. **f**, **g**, Frequency of Ca^{2+} transients in *tdc2*^{RO54}, *tβh*^{nM18} (**f**, $n = 6$, 96 cells total) and *Oct-TyrR*^{hono} mutants (**g**, n listed for each genotype, 16 cells randomly selected and analysed for each sample). **h**, Chemotaxis assay ($n = 12$). **i**, Gentle touch assay ($n = 30$). $^{*}P < 0.05$, $^{**}P < 0.01$; NS, not significant; error bars, s.e.m. **c**, **d**, Paired t-test; **b**, **f**–**i**, one-way ANOVA followed by Tukey's *post hoc* test.

elevation in astrocytes and silencing of dopaminergic neurons (Fig. 3c and Extended Data Fig. 2k). These data indicate that Tyr signals through astrocyte Oct-TyrR and Wtrw to inhibit downstream dopaminergic neuron activity.

To investigate how modulation of dopaminergic neurons regulates larval chemotaxis behaviour, we performed a series of acute manipulations. We first expressed the temperature-sensitive channel TrpA1 in dopaminergic neurons; after 24-h ectopic activation of dopaminergic neurons, larvae exhibited profound chemotaxis defects similar to those observed when Wtrw or Oct-TyrR were depleted from astrocytes (Extended Data Fig. 2h). In addition, feeding larvae a dopamine D1-like receptor antagonist rescued deficits associated with *wtrw*^{RNAi} in astrocytes in chemotaxis assays (Extended Data Fig. 2i). These data support the notion that the increased dopaminergic neuron activity observed after depletion of astrocytic Oct-TyrR and Wtrw is responsible for defects in chemotaxis behaviour.

How do astrocytes regulate dopaminergic neuron firing? Astrocytic release of ATP and signalling through purinergic receptors is one mechanism by which astrocytes appear to modulate neuronal activity[27,28]. The *Drosophila* genome contains a single seven-transmembrane-domain purinergic receptor, AdoR, that is most similar to mammalian adenosine receptors[29]. Pretreatment of larval CNS preparations with the AdoR antagonist SCH-442416 blocked Tyr-induced silencing of dopaminergic neurons without altering overall dopaminergic neuron activity before Tyr treatment. Similar results were observed in AdoR null mutants (Fig. 4a and Extended Data Fig. 2j). Purinergic signalling often results from vesicular release of ATP, which can be hydrolysed to adenosine by ectoenzymes. We manipulated exocytosis selectively in astrocytes using a dominant-negative version of the dynamin Shibire (Shi^{DN}) and found that this suppressed the ability of Tyr to silence dopaminergic neurons. This blockade was not enhanced further by application of AdoR antagonists and had no effect on baseline dopaminergic neuron activity before Tyr treatment (Fig. 4b and Extended Data Fig. 2l). Finally, to determine whether astrocyte Ca^{2+} signalling through TRP channels is sufficient to suppress dopaminergic neuron firing, we expressed the wasabi (AITC)-sensitive *Drosophila* TrpA1 channel in astrocytes and tested the effects of AITC application on astrocytic Ca^{2+} signalling and dopaminergic neuron firing. Exposure of control preparations to AITC did not alter astrocyte Ca^{2+} levels, but application of AITC to preparations expressing TrpA1 in astrocytes led to an increase in astrocytic GCaMP6s signals of around 20% (Extended Data Fig. 2m), similar to that elicited by Tyr application (Fig. 1d). Moreover, activation of astrocyte Ca^{2+} signalling by AITC resulted in strong suppression of dopaminergic neuron activity. This effect was reversed by application of AdoR antagonists and did not occur when AITC was applied to control (that is, non-TrpA1 expressing) preparations (Fig. 4c and Extended Data Fig. 2n). Thus TrpA1 channel-mediated increases in astrocytic Ca^{2+} signalling are sufficient to silence

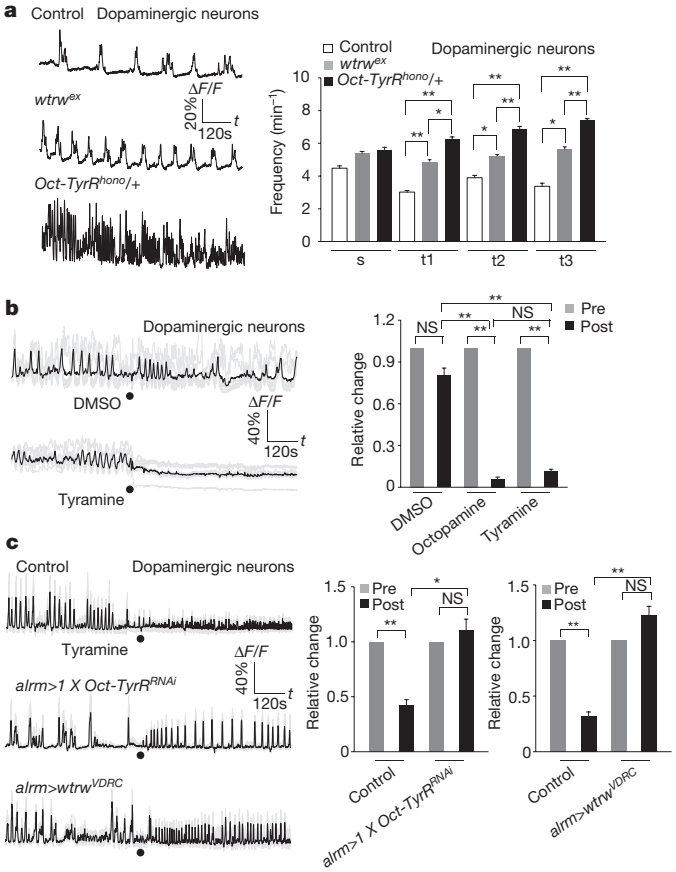

Figure 3 | Astrocytes mediate Tyr-induced inhibition of dopaminergic neurons through Oct-TyrR. a, Enhanced activity of dopaminergic neurons in *wtrw*^{ex} mutant and *Oct-TyrR*$^{hono/+}$ heterozygote larvae ($n = 10$; 80 neurites). s, subesophageal segments; t, thoracic segments. **b**, Tyr and Oct (2.5 mM) inhibit the activity of dopaminergic neurons ($n = 6$; 48 neurites). **c**, Astrocyte-specific RNAi for *Oct-TyrR* or *wtrw* attenuates inhibition of dopaminergic neurons by Tyr ($n = 6$; 48 neurites). Black dots, points at which Tyr was perfused. $*P < 0.05$, $**P < 0.01$; NS, not significant; error bars, s.e.m. **b**, **c**, Paired *t*-test (**b**, same treatment; **c**, same genotype); **a**–**c**, one-way ANOVA followed by Tukey's *post hoc* test.

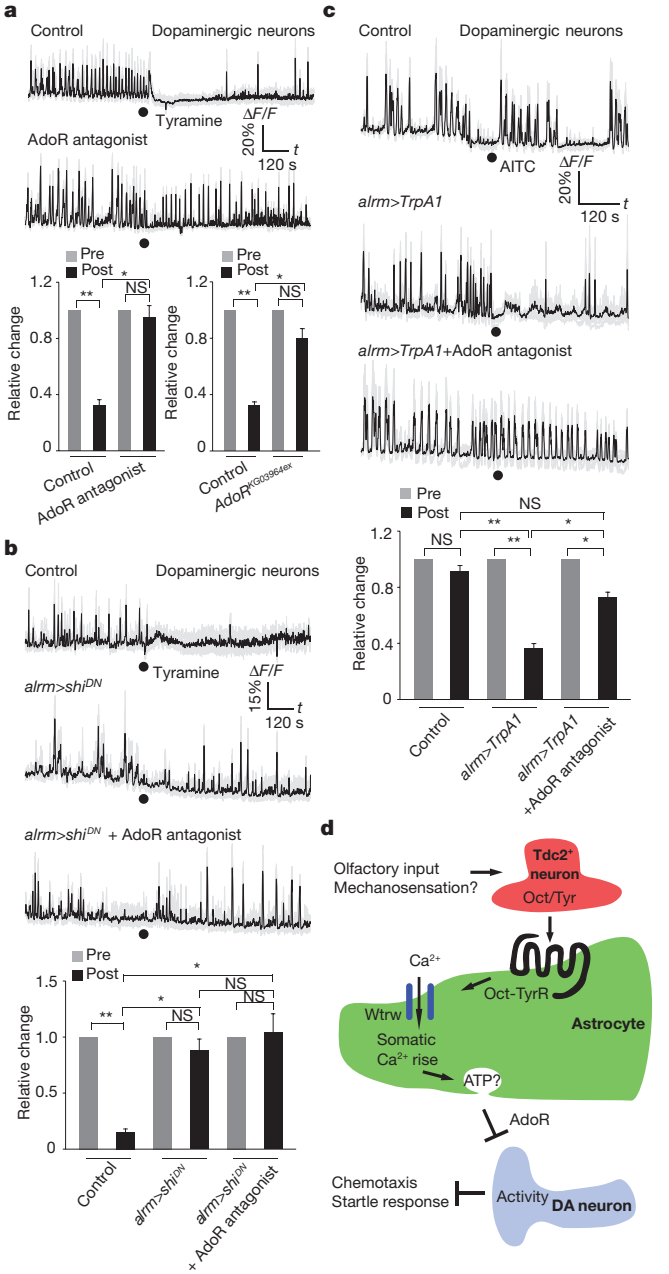

Figure 4 | Tyr-mediated inhibition of dopaminergic neurons depends on adenosine receptors and glial endocytic function. a, AdoR is required for Tyr-mediated inhibition of dopaminergic neurons ($n = 6$; 48 neurites). **b**, Blockade of endocytic function by dominant-negative shibire (*shi*^{DN}) attenuates inhibition of dopaminergic neurons by Tyr ($n = 6$; 48 neurites). Black dots, points at which Tyr was perfused. **c**, Ca^{2+} influx to astrocytes through TrpA1 is sufficient to inhibit dopaminergic neurons ($n = 6$; 48 neurites). Black dots, points at which AITC was perfused. **d**, Model. Olfactory and (probably) mechanosensory information flow towards Tdc2^{+} neurons, which release Oct and Tyr to activate Oct-TyrR on astrocytes and in turn induce astrocytic Ca^{2+} entry through the TRP channel Wtrw. The increase in astrocytic Ca^{2+} is sufficient to silence dopaminergic (DA) neurons through a mechanism requiring the adenosine receptor AdoR, potentially through astrocyte ATP release and its breakdown to adenosine. Inhibition of dopaminergic neuron activity by astrocytes is essential for normal chemotaxis and startle-induced reversal. $*P < 0.05$, $**P < 0.01$; NS, not significant; error bars, s.e.m. **a**–**c**, Paired *t*-test (same genotype); Wilcoxon and Mann–Whitney tests followed by Bonferroni-Holm *post hoc* test (**a**, **b**); one-way ANOVA followed by Tukey's *post hoc* test (**c**).

dopaminergic neurons *in vivo*. Silencing of dopaminergic neurons is likely to be mediated by release of ATP from astrocytes and subsequent activation of AdoR on dopaminergic neurons.

It has been assumed that neuromodulators alter neural circuit activity and behaviour by acting directly on neurons; however, astrocytes (and other glia) express a diverse array of neuromodulatory receptors, suggesting they may contribute to the global effects of these neurotransmitters. In this study we have demonstrated that neuromodulatory signalling in at least some cases flows through astrocytes. We have shown that *Drosophila* astrocytes exhibit robust Ca^{2+} signalling events that are remarkably similar to those observed in awake behaving mice[14–16]. Similar to the global activation of astrocyte Ca^{2+} signalling by norepinephrine in mammals, release of Tyr (and probably Oct) *in vivo* triggers synchronous activation of astrocytes. We have identified Wtrw and Oct-TyrR as key components of the astrocyte Ca^{2+} signalling axis, and their loss-of-function phenotypes have provided direct evidence that astrocytic Ca^{2+} signalling modulates animal behaviour. Furthermore, we have shown that, during suppression of dopaminergic neuron activity, Oct and Tyr signal directly to astrocytes, and astrocyte Ca^{2+} transients execute neuromodulatory events downstream (Fig. 4d). Oct and Tyr have been linked to arousal and aggression in insects and are considered to be functionally equivalent to norepinephrine in mammals. The profound modulation of astrocytic Ca^{2+} levels by norepinephrine in mammals[14–16] suggests that activation of

astrocytic Ca^{2+} signalling by Tyr, Oct or norepinephrine, and in turn astrocyte-based neuromodulation, are ancient features of the metazoan nervous system. A reassessment of the cellular basis of neuromodulation is therefore warranted, with further reflection on direct roles for astrocytes in transducing neuromodulatory signals in neural circuits.

Online Content Methods, along with any additional Extended Data display items and Source Data, are available in the online version of the paper; references unique to these sections appear only in the online paper.

Received 22 October 2015; accepted 7 October 2016.
Published online 9 November 2016.

1. Cornell-Bell, A. H., Finkbeiner, S. M., Cooper, M. S. & Smith, S. J. Glutamate induces calcium waves in cultured astrocytes: long-range glial signaling. *Science* **247,** 470–473 (1990).
2. Charles, A. C., Merrill, J. E., Dirksen, E. R. & Sanderson, M. J. Intercellular signaling in glial cells: calcium waves and oscillations in response to mechanical stimulation and glutamate. *Neuron* **6,** 983–992 (1991).
3. Dani, J. W., Chernjavsky, A. & Smith, S. J. Neuronal activity triggers calcium waves in hippocampal astrocyte networks. *Neuron* **8,** 429–440 (1992).
4. Smith, S. J. Do astrocytes process neural information? *Prog. Brain Res.* **94,** 119–136 (1992).
5. Khakh, B. S. & McCarthy, K. D. Astrocyte calcium signaling: from observations to functions and the challenges therein. *Cold Spring Harb. Perspect. Biol*. **7,** a020404 (2015).
6. Araque, A. *et al.* Gliotransmitters travel in time and space. *Neuron* **81,** 728–739 (2014).
7. Khakh, B. S. & Sofroniew, M. V. Diversity of astrocyte functions and phenotypes in neural circuits. *Nat. Neurosci.* **18,** 942–952 (2015).
8. Fatatis, A. & Russell, J. T. Spontaneous changes in intracellular calcium concentration in type I astrocytes from rat cerebral cortex in primary culture. *Glia* **5,** 95–104 (1992).
9. Nett, W. J., Oloff, S. H. & McCarthy, K. D. Hippocampal astrocytes in situ exhibit calcium oscillations that occur independent of neuronal activity. *J. Neurophysiol.* **87,** 528–537 (2002).
10. Porter, J. T. & McCarthy, K. D. Hippocampal astrocytes in situ respond to glutamate released from synaptic terminals. *J. Neurosci.* **16,** 5073–5081 (1996).
11. Nimmerjahn, A., Mukamel, E. A. & Schnitzer, M. J. Motor behavior activates Bergmann glial networks. *Neuron* **62,** 400–412 (2009).
12. Doherty, J., Logan, M. A., Taşdemir, O. E. & Freeman, M. R. Ensheathing glia function as phagocytes in the adult *Drosophila* brain. *J. Neurosci.* **29,** 4768–4781 (2009).
13. Liu, L. *et al. Drosophila* hygrosensation requires the TRP channels water witch and nanchung. *Nature* **450,** 294–298 (2007).
14. Ding, F. *et al.* α1-Adrenergic receptors mediate coordinated Ca2+ signaling of cortical astrocytes in awake, behaving mice. *Cell Calcium* **54,** 387–394 (2013).
15. Paukert, M. *et al.* Norepinephrine controls astroglial responsiveness to local circuit activity. *Neuron* **82,** 1263–1270 (2014).
16. Srinivasan, R. *et al.* Ca^{2+} signaling in astrocytes from $Ip3r2^{-/-}$ mice in brain slices and during startle responses *in vivo*. *Nat. Neurosci.* **18,** 708–717 (2015).
17. Zhou, Y., Cameron, S., Chang, W.-T. & Rao, Y. Control of directional change after mechanical stimulation in *Drosophila*. *Mol. Brain* **5,** 39–52 (2012).
18. Shigetomi, E., Jackson-Weaver, O., Huckstepp, R. T., O'Dell, T. J. & Khakh, B. S. TRPA1 channels are regulators of astrocyte basal calcium levels and long-term potentiation via constitutive D-serine release. *J. Neurosci.* **33,** 10143–10153 (2013).
19. Duffy, S. & MacVicar, B. A. Adrenergic calcium signaling in astrocyte networks within the hippocampal slice. *J. Neurosci.* **15,** 5535–5550 (1995).
20. Salm, A. K. & McCarthy, K. D. Norepinephrine-evoked calcium transients in cultured cerebral type 1 astroglia. *Glia* **3,** 529–538 (1990).
21. Vömel, M. & Wegener, C. Neuroarchitecture of aminergic systems in the larval ventral ganglion of *Drosophila melanogaster*. *PLoS One* **3,** e1848 (2008).
22. Nitabach, M. N., Sheeba, V., Vera, D. A., Blau, J. & Holmes, T. C. Membrane electrical excitability is necessary for the free-running larval *Drosophila* circadian clock. *J. Neurobiol.* **62,** 1–13 (2005).
23. Saudou, F., Amlaiky, N., Plassat, J. L., Borrelli, E. & Hen, R. Cloning and characterization of a *Drosophila* tyramine receptor. *EMBO J.* **9,** 3611–3617 (1990).
24. Robb, S. *et al.* Agonist-specific coupling of a cloned *Drosophila* octopamine/tyramine receptor to multiple second messenger systems. *EMBO J.* **13,** 1325–1330 (1994).
25. Kutsukake, M., Komatsu, A., Yamamoto, D. & Ishiwa-Chigusa, S. A tyramine receptor gene mutation causes a defective olfactory behavior in *Drosophila melanogaster*. *Gene* **245,** 31–42 (2000).
26. Burke, C. J. *et al.* Layered reward signalling through octopamine and dopamine in *Drosophila*. *Nature* **492,** 433–437 (2012).
27. Newman, E. A. Glial cell inhibition of neurons by release of ATP. *J. Neurosci.* **23,** 1659–1666 (2003).
28. Lalo, U., Rasooli-Nejad, S. & Pankratov, Y. Exocytosis of gliotransmitters from cortical astrocytes: implications for synaptic plasticity and aging. *Biochem. Soc. Trans.* **42,** 1275–1281 (2014).
29. Brody, T. & Cravchik, A. *Drosophila melanogaster* G protein-coupled receptors. *J. Cell Biol.* **150,** F83–F88 (2000).

Supplementary Information is available in the online version of the paper.

Acknowledgements We thank our colleagues, the Vienna *Drosophila* RNAi Center and the Bloomington Stock Center for providing fly stocks, members of the Freeman laboratory for comments on the manuscript and A. Sheehan for generating the *wtrw::gfp* construct. This work was supported by NINDS grant R01 NS053538 (to M.R.F.). During the period of this study M.R.F. was an Investigator with the Howard Hughes Medical Institute.

Author Contributions Z.M. and M.R.F. designed experiments. Z.M. performed all experiments. T.S. provided *alrm-LexA::GAD* transgenic flies. D.E.B. provided unpublished data on norepinephrine-mediated activation of mammalian astrocytes and input that helped guide the course of the study. Z.M. and M.R.F. wrote the manuscript with editing by T.S.

Author Information Reprints and permissions information is available at www.nature.com/reprints. The authors declare no competing financial interests. Readers are welcome to comment on the online version of the paper. Correspondence and requests for materials should be addressed to M.R.F. (freemmar@ohsu.edu).

Reviewer Information *Nature* thanks L. Luo, B. MacVicar, L. Vosshall and the other anonymous reviewer(s) for their contribution to the peer review of this work.

METHODS

Fly stocks and husbandry. Flies were cultured in standard cornmeal food at 25 °C in 12 h–12 h light–dark cycles. Fly stocks include: *w*^{1118}, *alrm-Gal4*, *alrm-LexA::GAD*, *UAS-wtrw-gfp*, *LexAop-R-GECO1* (Bloomington, 52224), *tdc2-Gal4* (Bloomington, 9313), *20XUAS-IVS-GCaMP6s* (Bloomington, 42746), *13XLexAop2-IVS-GCaMP6s-p10* (Bloomington, 44274), *UAS-Kir2.1-EGFP* (Bloomington, 6595), *UAS-Oct-TyrR*^{RNAi} (Bloomington, 28332), *th-Gal4* (Bloomington, 8848), *UAS-wtrw*^{VDRC} (VDRC, 107423), *Oct-TyrR*^{hono} (Kyoto, 109038), *UAS-shi*^{DN} (Bloomington, 5822), *UAS-TrpA1* (Bloomington, 26263), *UAS-NpHR* (Kyoto, 117008), *UAS-CsChrimson* (Bloomington, 55135), *AdoR*^{KG03964ex} (Bloomington, 30868), *tdc2-LexA::p65* (ref. 26), *UAS-wtrw*$^{2.23}$ (ref. 13), *wtrw*^{ex} (ref. 30), *tβh*^{nM18} (ref. 31), *tdc2*^{RO54} (ref. 32), *th-LexA::p65* (ref. 33), *tsh-Gal80* (ref. 34).

Chemotaxis and light avoidance. These two assays were performed using protocols described previously with minor modifications[35]. Briefly, pools of ~100 3rd instar larvae (108–120 h after egg lay) were allowed to move freely for 5 min on Petri dishes with according settings for chemotaxis assay or phototaxis assay, then the numbers of larvae in odorant versus vehicle circles or in light versus dark quadrants were scored, respectively. Response indices were calculated as: $RI_{chemotaxis} = (N_{odor} - N_{vehicle})/(N_{odor} + N_{vehicle})$; $RI_{light\ avoidance} = (N_{dark} - N_{light})/(N_{dark} + N_{light})$. IAA was diluted to 1:5,000 in mineral oil, and pure mineral oil was used as the control. Light intensity in phototaxis assays was 2,400 lx white light (5,400 K). Thermogenetic manipulation of dopaminergic neurons was accomplished by transferring 3rd instar larvae from 18 °C to 25 °C to allow activation of TrpA1 for 24 h before testing. For chemotaxis assays related to D1-like or D2-like dopamine receptor inhibitors, 3rd instar larvae were fed on cornmeal food mixed with inhibitors for 24 h before testing.

Gentle touch assay. We struck early 3rd instar larvae (84–96 h after egg lay) in the thoracic segments with a hair while they were moving straight. No response, a stop, head retraction and turn were grouped into type I responses, and initiation of at least one single full body retraction or multiple full body retractions were categorized as type II reversal responses.

Larval motility. Third instar larvae (108−120 h after egg lay) were videotaped and the maximal velocity was calculated by dividing the travel distance measured when larvae moved straight without pause by the time taken.

Molecular biology and transgenic flies. *pUAST-wtrw::gfp* was made by cloning full length *wtrw* tagged with *gfp* at its C-terminal into *pUAST*. Transgenic flies were obtained by standard germline injection (BestGene Inc.).

Chemicals, buffers and antibodies. For live preparation studies, all chemicals were diluted in live imaging buffer (110 mM NaCl, 5.4 mM KCl, 1.2 mM $CaCl_2$, 0.8 mM $MgCl_2$, 10 mM D-glucose, 10 mM HEPES, pH adjusted to 7.2), including 1 μM tetrodotoxin (TTX), 0.1 mM lanthanum chloride ($LaCl_3$), 2.5 mM Oct, 2.5 mM glutamate, 2.5 mM acetylcholine, 2.5 mM GABA, 150 μM AITC, 10 μM SCH-442416, 1 mM terazosin and 0.5 mM Tyr unless otherwise stated. The concentration of SCH-23390 (dopamine D1-like receptor antagonist) was 0.2 mg/ml; eticlopride (dopamine D2-like receptor antagonist) was 0.2 mg/ml; all-*trans* retinal was 10 mM. Rabbit anti-GAT antibody was used at 1:5,000 and mouse anti-nc82 antibody was used at 1:50 (DSHB).

Live imaging and data analysis. First instar larvae were immersed in halocarbon oil 27 and immobilized between coverslips and slides to image the activity of neurons and astrocytes through the cuticle in intact larvae. Third instar wandering stage larvae were used to dissect the CNS. Briefly, intact CNSs were transferred to a silicone filled dish after dissection and incubated with 100 μl live imaging buffer. Samples were allowed to sit at room temperature for 15 min before imaging. To examine the effects of $LaCl_3$ or tetrodotoxin on calcium transients, samples were pre-incubated in buffer containing chemicals for 15 min before imaging. Movies were acquired by using Volocity software on a spinning disc microscope equipped with a 20× (dissected CNS) or 40× (intact larvae) water immersion objective at 2 frames per s. Changes in GCaMP intensity of ROIs were calculated and expressed as $(F_{t1\ldots n} - F)/F$ (first 10 frames were averaged as F), which then were plotted over time. Plotted traces were semi-automatically analysed by the multiple peak fitting function of Igor Pro (WaveMetrics Inc.) to obtain the numbers and amplitudes of peaks.

Bath application of drugs. Samples were prepared as described above and incubated with imaging buffer (with/without 1 μM TTX). At ~240 s (astrocytes) or ~300 s (neurons) after imaging, 100 μl live imaging buffer containing 2× final concentrations of chemicals (with/without 1 μM TTX) were directly added to the medium, and imaging continued. The GCaMP6s intensity of ROIs was plotted and analysed as mentioned above. For terazosin experiments we first examined preparations for 6 min (control, pre-exposure window). Then terazosin was perfused for 3 min, and we then imaged for an additional 6 min (exposed window). Data points of 6–9 min that represented the perfusion window were omitted from the graph.

Optogenetic activation and inactivation of neurons. For CsChrimson activation of olfactory neurons, larvae were grown on cornmeal food daily topped with 100 μl all-*trans* retinal for 3 days. Early 3rd instar larvae were immobilized between coverslips and slides in halocarbon oil 27 and the activity of $Tdc2^+$ neurons reflected by GCaMP6s was continuously monitored except when red light (640 nm, 3.41 mW/mm^2) was delivered through an epifluorescence light source. Halorhodopsin-mediated inhibition of $Tdc2^+$ neurons was accomplished by growing larvae on cornmeal food topped daily with 100 μl all-*trans* retinal for 4–5 days. Larval brains were dissected from wandering 3rd instar larvae and prepared as described above for imaging somatic calcium transients in astrocytes. GCaMP6s signals were recorded for 6 min, then halorhodopsin was activated (within ~30 s) by alternating delivery of 561 nm (0.26 mW/mm^2, 3 s, for photoinhibition) and blue light 488 nm (500 ms, for imaging GCaMP6s-labelled astrocytes) for another 6 min. Data points from two consecutive movies were then assembled together to show changes in somatic calcium transients.

Statistical analysis. No statistical methods were used to predetermine sample size. All *n* numbers represent biological replicates. Data were pooled from 2–3 independent experiments. The experiments were not randomized or blinded. The Shapiro–Wilk test (normal distribution if $P > 0.05$) was used to determine the normality of data. Statistical comparisons were performed using one-way ANOVA followed by Tukey's *post hoc* test or paired Student's *t*-test (two-tailed). Non-normally distributed data were compared using Wilcoxon and Mann–Whitney tests followed by Bonferroni-Holm *post hoc* test. $P < 0.05$ was considered significant. All the data in bar graphs are expressed as mean ± s.e.m.

30. Kim, S. H. *et al. Drosophila* TRPA1 channel mediates chemical avoidance in gustatory receptor neurons. *Proc. Natl Acad. Sci. USA* **107,** 8440–8445 (2010).
31. Monastirioti, M., Linn, C. E., Jr & White, K. Characterization of *Drosophila* tyramine β-hydroxylase gene and isolation of mutant flies lacking octopamine. *J. Neurosci.* **16,** 3900–3911 (1996).
32. Cole, S. H. *et al.* Two functional but noncomplementing *Drosophila* tyrosine decarboxylase genes: distinct roles for neural tyramine and octopamine in female fertility. *J. Biol. Chem.* **280,** 14948–14955 (2005).
33. Galili, D. S. *et al.* Converging circuits mediate temperature and shock aversive olfactory conditioning in *Drosophila*. *Curr. Biol.* **24,** 1712–1722 (2014).
34. Clyne, J. D. & Miesenböck, G. Sex-specific control and tuning of the pattern generator for courtship song in *Drosophila*. *Cell* **133,** 354–363 (2008).
35. Lilly, M. & Carlson, J. smellblind: a gene required for *Drosophila* olfaction. *Genetics* **124,** 293–302 (1990).

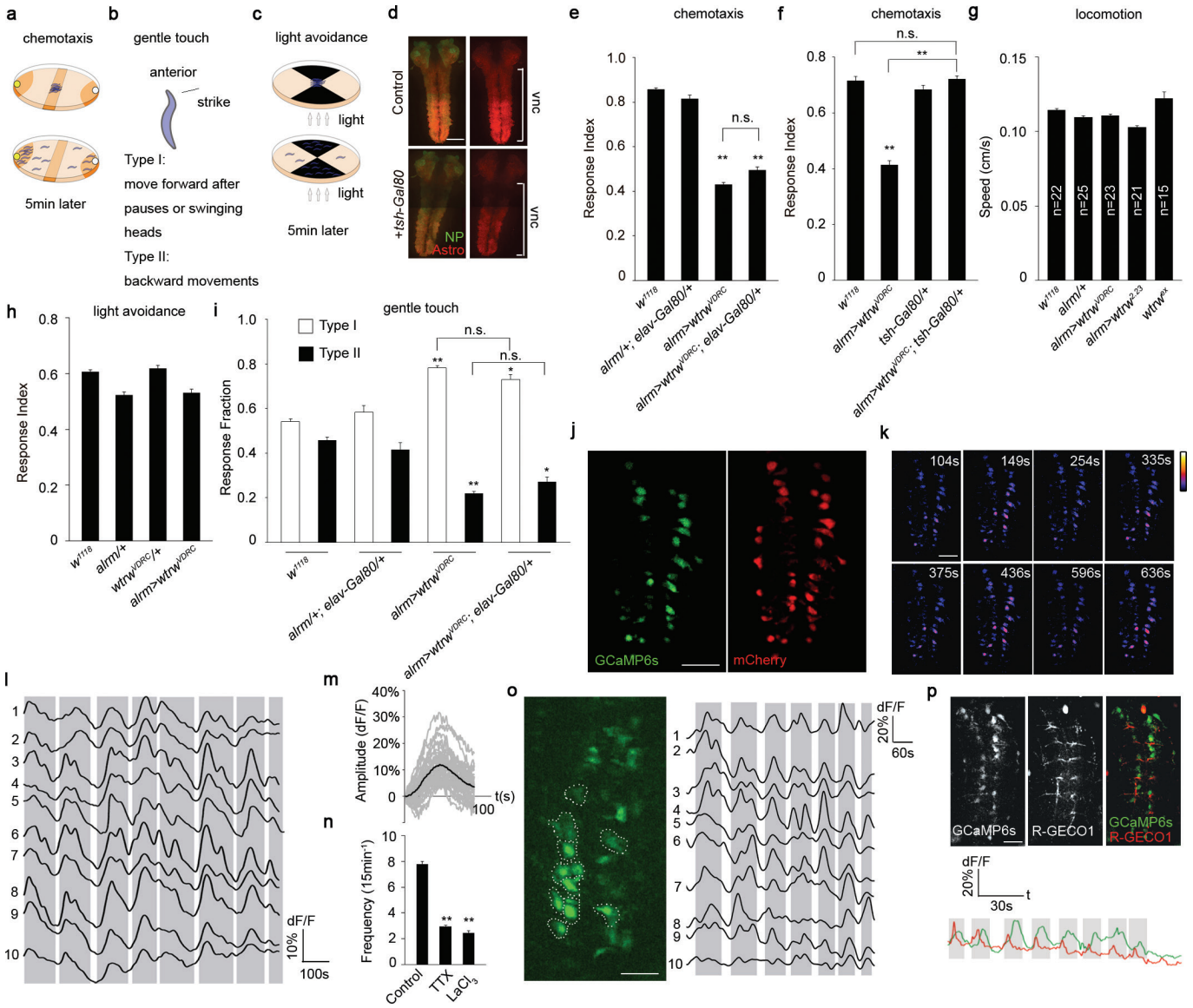

Extended Data Figure 1 | Synchronous somatic Ca^{2+} transients in *Drosophila* astrocytes. a–c, Brief diagrams of behavioural tests. **d**, *tsh-Gal80* suppression of *alrm-Gal4* activity. Nc82, neuropil (NP). Astrocytes (Astro), *alrm > myr::tdTomato*. Vnc, ventral nerve cord. Scale bar, 50 μm. **e**, **f**, Chemotaxis assay ($n = 12$). **g**, Locomotion assay (*n* listed). **h**, Light avoidance assay ($n = 12$). **i**, Gentle touch assay ($n = 24$). **j**, GCaMP6s and mCherry expression in astrocytes. Scale bar, 50 μm. **k**, Representative pseudocoloured images of four continuous Ca^{2+} transients. Scale bar, 50 μm. **l**, Traces of normalized GCaMP6s intensity over mCherry of 10 individual astrocytes in 15-min live imaging windows. **m**, Averaged traces of individual somatic Ca^{2+} transients. **n**, Somatic Ca^{2+} transients in astrocytes treated with TTX and $LaCl_3$ ($n = 10$, 160 cells). **o**, GCaMP6s expression in astrocytes and traces of 10 individual astrocytes from an intact larva. Scale bar, 20 μm. Grey bars (**l**, **o**) represent population rise or fall in GCaMP6s signals. **p**, GCaMP6s-labelled astrocytes and R-GECO1-labelled $Tdc2^{+}$ neurites and their averaged traces in an intact larva. Scale bar, 20 μm. $*P < 0.05$, $**P < 0.01$; NS, not significant; error bars, s.e.m. Wilcoxon and Mann–Whitney tests followed by Bonferroni-Holm *post hoc* test (**e**, **n**), one-way ANOVA followed by Tukey's *post hoc* test (**f**–**i**).

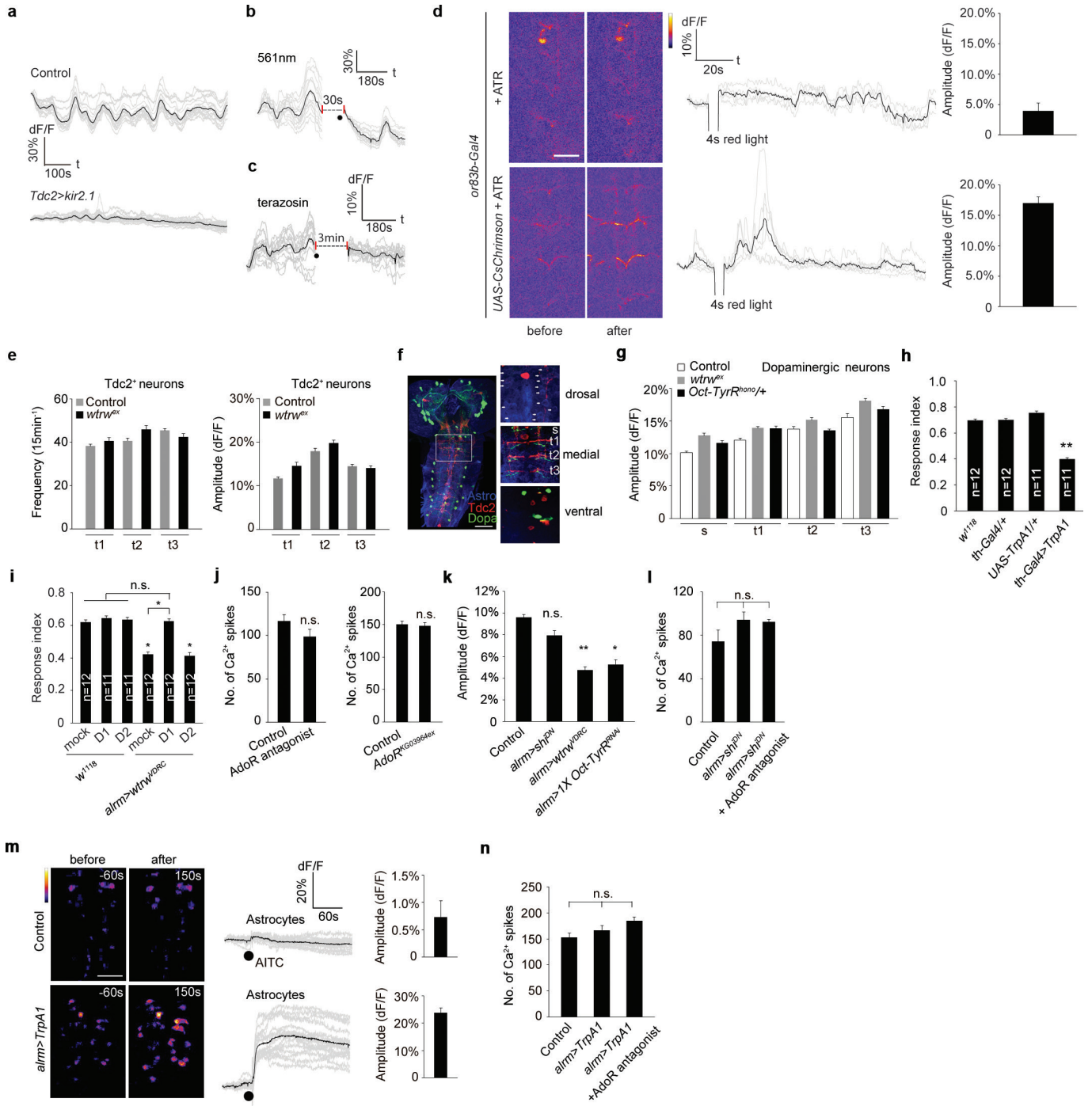

Extended Data Figure 2 | Somatic Ca^{2+} transients in astrocytes inhibit the activity of dopaminergic neurons. **a**–**c**, Representative traces of astrocyte Ca^{2+} transients with blockade of Tyr and Oct signalling. **d**, Stimulation of olfactory neurons activates $Tdc2^+$ neurons ($n = 3$–4). Scale bar, 25 μm. **e**, Activity of $Tdc2^+$ neurons is not altered in *wtrw* mutants ($n = 8$, 48 neurites). **f**, Astrocytes, $Tdc2^+$ neurons and dopaminergic neurons in larval CNS. Dorsal (arrows point to astrocyte somas labelled with anti-GAT antibody), medial (neurites intermingled with ramified processes of astrocytes for monitoring activity are labelled) and ventral (cell bodies of tdc2>myr::tdTomato, Gal4/UAS and th>GCaMP6s LexA/LexAop dopaminergic neurons) images from the boxed region are shown (right). s, subesophageal. t, thoracic. Scale bar, 50 μm. **g**, Amplitude of Ca^{2+} spikes in dopaminergic neurons ($n = 10$, 80 neurites). **h**, **i**, Chemotaxis assay (n listed). **j**, Number of Ca^{2+} spikes of dopaminergic neurons ($n = 6$, 48 neurites). **k**, Responses of astrocytes to Tyr (0.5 mM) in the presence of TTX ($n = 6$, 96 cells total). **l**, Number of Ca^{2+} spikes in dopaminergic neurons ($n = 6$, 48 neurites). **m**, AITC induces Ca^{2+} influx into astrocytes expressing TrpA1 ($n = 5$, 80 cells). Scale bar, 50 μm. **n**, Number of Ca^{2+} spikes in dopaminergic neurons ($n = 6$, 48 neurites). $^*P < 0.05$, $^{**}P < 0.01$; NS, not significant; error bars, s.e.m. One-way ANOVA followed by Tukey's *post hoc* test.